Second-day road log from Los Alamos through Valles Caldera and return

Jamie N. Gardner, Fraser Goff, and Margaret Ann Rogers

1996, pp. 41-58. https://doi.org/10.56577/FFC-47.41

in:

Jemez Mountains Region, Goff, F.; Kues, B. S.; Rogers, M. A.; McFadden, L. S.; Gardner, J. N.; [eds.], New Mexico Geological Society 47th Annual Fall Field Conference Guidebook, 484 p. https://doi.org/10.56577/FFC-47

This page is intentionally left blank to maintain order of facing pages.

SECOND-DAY ROAD LOG, FROM LOS ALAMOS THROUGH VALLES CALDERA AND RETURN

JAMIE N. GARDNER, FRASER GOFF and MARGARET ANNE ROGERS

FRIDAY, SEPTEMBER 27, 1996

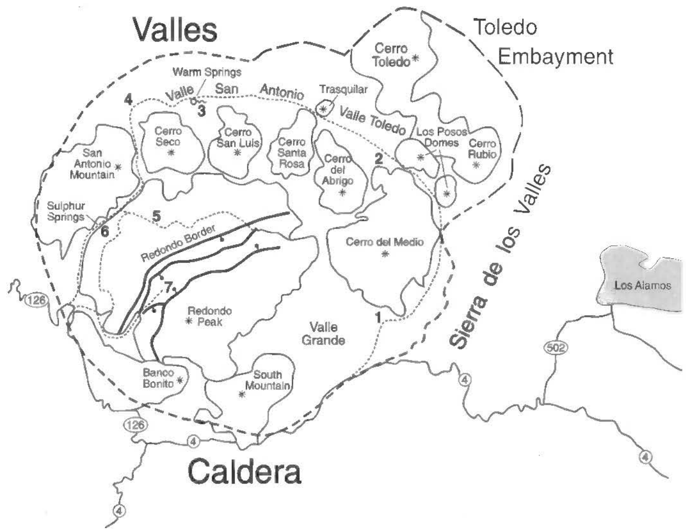

Assembly point: Sullivan Field, Diamond Drive, Los Alamos
Departure time: 7:00 a.m.
Distance: 52.1 miles
Stops: 7

Summary

The second day of the field conference examines the heart of Valles caldera, the world's type resurgent caldera and host to a classic liquid-dominated geothermal system. Our route will take us from Los Alamos through the pre-caldera volcanic highland of the Sierra de los Valles to the northeast edge of the Valle Grande (Stop 1). This viewpoint allows us to summarize basic information on the caldera and a chance to peer at a post-Valles moat rhyolite. From there we will drive north into Valle Toledo to view the Toledo embayment (Stop 2) and discuss the geology of the northern caldera wall. We continue west into Valle San Antonio to examine hydromagmatic deposits at Warm Springs dome, an eruptive remnant of the Toledo ring-fracture (Stop 3). Farther west, we will look at relatively unstudied, intracaldera lacustrine deposits that are so widespread in Valle San Antonio (Stop 4). Next we head south between Cerro Seco and San Antonio Mountain moat rhyolites to Alamo Canyon bog on the west side of Redondo border (Stop 5). This site gives us our first glimpse of hydrothermal features and the complexity of resurgent dome geology. From this site, we drive south to Sulphur Springs (Stop 6) where we can examine in detail acid hot springs and fumaroles and discuss subsurface geology. We finish the day with a drive into Redondo Creek to examine the geology of the keystone graben of the resurgent dome (Stop 7). We thank Heddy Dunn and Georgia Strickfaden of the Los Alamos Historical Society for some of the comments provided for the first 14 mi of the road log.

Mileage

0.0 Start mileage at Sullivan Field (high school football stadium) parking lot, intersection of Diamond Drive and Canyon Road, Los Alamos; head south on Diamond (right turn from parking lot at light); pass through traffic light at intersection of Diamond and Trinity Drive. **0.1**

0.1 Stay in right traffic lane. Emergency room entrance to Los Alamos Medical Center on left at light. **0.3**

0.4 Stay in right traffic lane. Cross Omega Bridge and Los Alamos Canyon fault. Omega Bridge was built in 1951 and was the highest and longest span in the state when built. Before the bridge was built, traffic traveled through the canyon on a tortuous old ranch road. The Lab's main facilities relocated to their present locale on this mesa after World War II. The bridge connected the expanding laboratory with the growing residential area on the mesa to the immediate north. **0.1**

0.5 Take right turning lane (west) onto West Jemez Road (NM-501) at south end of bridge; yield to westbound traffic on West Jemez Road; pass fire station on right and Technical Area (TA) 3, Los Alamos National Laboratory (LANL), on left. LANL was called the Los Alamos Laboratory during World War II when it was secretly established for its mission to create the first atomic bombs. At that time, the laboratory's main facilities and technical areas closely surrounded Ashley Pond in the heart of town where now one finds a park, the County Municipal Building, the Los Alamos Inn, and other commercial establishments. **0.1**

0.6 Pass through light at intersection of West Jemez Road with Casa Grande; LANL Administration Building on left. **0.2**

0.8 Pass through light at intersection of West Jemez Road with Pajarito Road **1.1**

1.9 On right, intersection with U. S. Forest Service (USFS) Road 1 (road to Pajarito Mountain Ski Area also known as Camp May Rd.); stay on West Jemez Road as it bends south and follows base of scarp of main trace of the Pajarito fault zone. Camp May was originally a summer and winter camp for the Los Alamos Ranch School, a private boy's prep-school which existed from 1917 to 1943 (see Chambers and Aldrich, this volume). Pajarito Mountain ski area, established in the late 1950s, is operated for public use by the Los Alamos Ski Club. It has 34 runs, 5 chair lifts and provides excellent intermediate to advanced skiing. **0.3**

2.2 On left, road to LANL technical areas TA-6, TA-8, TA-9, TA-14, TA-15, TA-22, TA-40, plus other TAs. **0.9**

3.1 On left, road to LANL technical areas TA-6 through TA-40. At one time this area was a private ranch called "Anchor Ranch" which, along with other ranches and homesteads, was taken by eminent domain by the government for use by the Manhattan Project. If one drives by slowly and looks to the left, one might catch a glimpse of an original ranch tank (pond) used as a swimming hole during the Manhattan Project and earlier times. Explosive testing was conducted here and at nearby "S-Site" by the Laboratory. **0.8**

3.9 On left, road to LANL technical areas TA-11, TA-16, TA-28 and TA-37. This area is known as "S-site" because it was at one time a sawmill and great piles of sawdust were found here when the Lab was in its early days. The lumber milled here was primarily cut in the Jemez Mountains and probably sent on by rail along the Rio Grande below Los Alamos. S-site was an assembly area for the World War II nuclear bombs, and is today the center of LANL's nuclear weapons program. **0.9**

4.8 Stop sign. Old guard station on right, Back Gate. Bandelier National Monument boundary sign across intersection. Turn right (west) onto NM-4; follow signs toward Jemez Springs and Cuba; begin to climb, through switchbacks, up steep hill on one fault scarp in the Pajarito fault zone. **0.3**

5.1 Hairpin turn on fault scarp. **0.4**

5.5 Road makes right-angle bend to west, leaving top of fault scarp; outcrops of densely welded Bandelier Tuff (Tshirege Member, Unit E) on right. **0.3**

5.8 Exposure on right of contact between units E and F of the upper Tshirege Member; sandy parting at contact is probably a surge deposit. **0.3**

6.1 On right, outcrops of unit F, Tshirege Member, Bandelier Tuff. **0.2**

6.3 On right, intersection with USFS-181, road to American and Armstead springs. **0.5**

6.8 Turnout on right to West Gate (former Girl Scout Camp and first ski area). This ski area, Sawyer's Hill, was first used in the days of the Los Alamos Ranch School. Some trails were cleared during the Manhattan Project days through use of high explosives supervised by George Kistiakowsky, the head of the Lab's explosives group. **0.7**

7.5 On right, Tschicoma Formation dacite in roadcuts. **0.3**

7.8 Entering Sandoval; leaving Los Alamos County, which was created in 1949 out of a chunk of Sandoval County. Los Alamos is still the state's smallest county (and probably has the state's highest per-capita income and education). **0.2**

8.0 Entering Bandelier National Monument. **0.1**

8.1 Views of Frijoles canyon on left; thick accumulations of Bandelier Tuff ponded in this low on the pre-Bandelier topography. **1.9**

10.0 Hairpin turn at head of Frijoles Canyon. Bandelier Tuff in roadcuts on right. **0.9**

10.9 On left, junction with USFS-289 (Dome Road). **0.7**

11.6 Leave Bandelier National Monument and begin descent down east caldera wall into collapse depression of Valles caldera. See Figure 2.1 for generalized geology of the caldera and vicinity. **0.8**

12.4 Small outcrops on left are Tschicoma Formation dacite. **0.4**

12.8 Valle Grande turnout on right. **0.6**

13.4 Rabbit Mountain dome (1.46 Ma) of the Cerro Toledo Rhyolite is visible to the SSW and is an aphyric, high-silica rhyolite (76–77 wt-% SiO_2) of post-Toledo caldera age (Smith et al., 1970; Stix et al., 1988). The dome sits outside the southeast structural margin of Valles caldera. Although smaller, Rabbit Mountain has similarities to the Rhyolite of Glass Mountain which sits on the northeast structural margin of the Long Valley (California) caldera, and also predates caldera formation (Bailey, 1989). **0.2**

13.6 **Turn hard right** to go through gate of Baca Land and Cattle Company; this property cannot be entered without permission. Continue north on dirt road that parallels NM-4; road crosses the Valle Grande, and travels across talus from the caldera walls and then alluvium.

The original land grant to the Baca family was for 5 plots of land, each 100,000 acres in size. One of the family's parcels was in Las Vegas, New Mexico, but a land swap was made for the Las Vegas parcel and the Baca Family's first choice for a swap was the Valle Grande land. Therefore, this 100,000 acre parcel was known as the "Baca Location #1." Frank Bond, an Española merchant and sheep man, purchased the Baca Location grant in 1906 to graze his flocks during the first half of this century. In 1960, the parcel was sold to the Dunigan family who kept the original land-grant name in its "Baca Land and Cattle Company" designation. The U.S. Department of the Interior asked for 4000 acres of the eastern edge of the parcel as it was geographically tied in with Bandelier National Monument. So the Dunigan's ranch is "only" 96,000 acres today. **0.7**

14.3 Cold pond on left. **0.2**

14.5 Valle Grande spring forms pond downhill on left that never freezes (always 12±2°C). Spring water is very low in tritium suggesting relatively deep circulation within the caldera-fill deposits (Vuataz and Goff, 1986). **0.5**

15.0 Cross small creeks forming part of the headwaters of the East Fork of the Jemez River. **0.3**

15.3 Small duck pond to right. **0.5**

15.8 Pass through old fence on left and corner of new fence on right; cross (normally) dry creek bed; skyline on the right is caldera rim, composed mostly of dacitic rocks of the Sierra de los Valles. **0.3**

16.1 **Turn hard right** at road junction and then park. **STOP 1. Valle Grande view and Cerro del Medio.** The lava at this hill is a post-Valles caldera moat rhyolite dome (Smith et al., 1970), part of the Valle Grande Member of the Valles Rhyolite. It is one of three mapped flow lobes from Cerro del Medio (Doell et al., 1968), most recently dated by Spell and Harrison (1993) at 1.133 to 1.095 Ma, and is a high-silica rhyolite (77 wt-% SiO_2). At this location, the rock is generally grey, devitrified, and spherulitic, having some flow-banding and pinkish oxidation. Phenocrysts consist of sparse quartz, sanidine, rare pyroxene and opaque oxides, and very rare hornblende. Cavities may contain vapor-phase tridymite and feldspar. On the north side of the

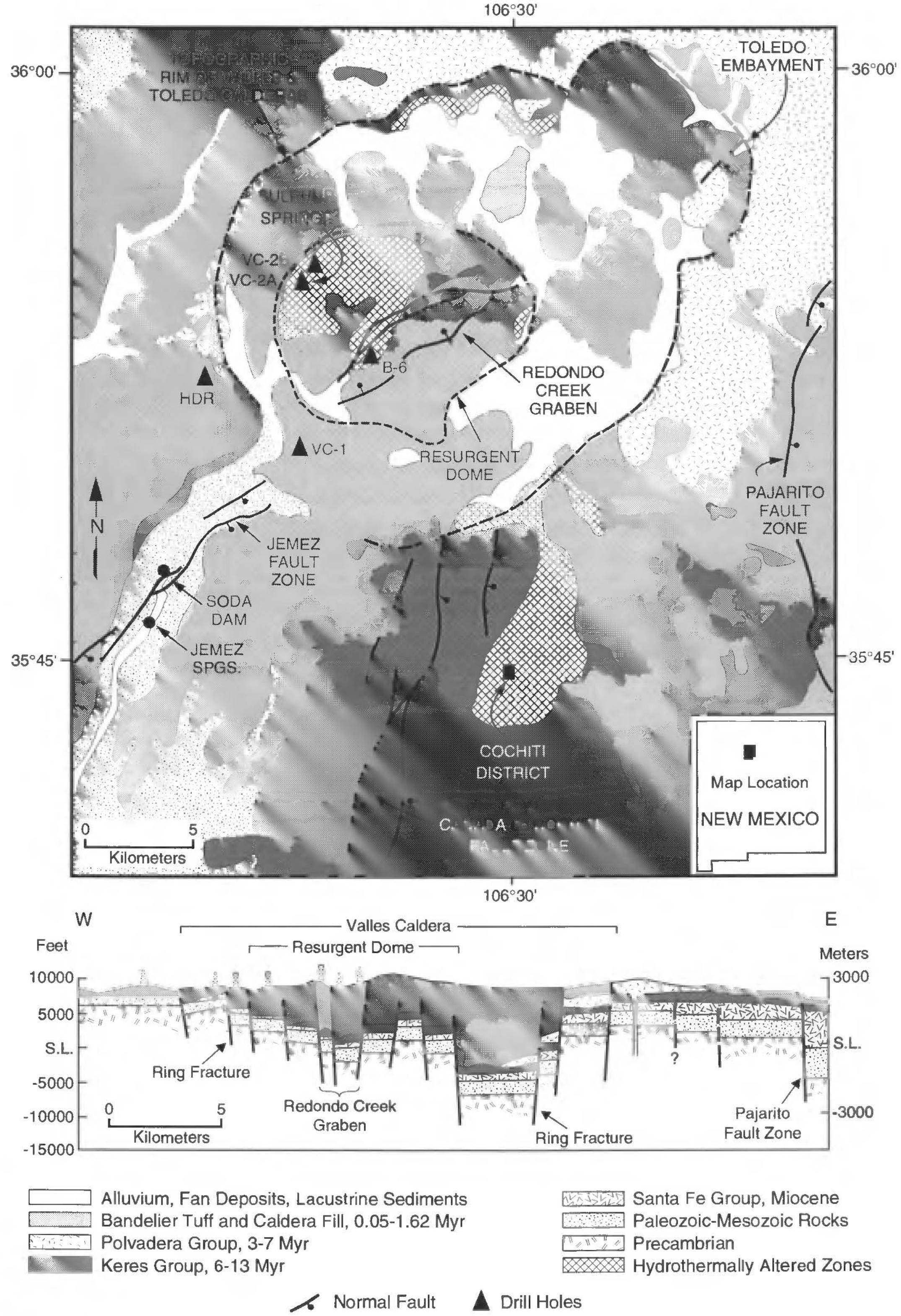

FIGURE 2.1. Generalized geologic map and cross section of the Valles caldera area (modified from Goff and Gardner, 1994).

dome, the rhyolite consists partially of jet black aphyric obsidian with occasional white spherulites.

Valles caldera formed 1.22 Ma (Izett and Obradovich, 1994) during catastrophic eruption of approximately 70 mi^3 of high-silica rhyolitic ignimbrite of the Tshirege Member, Bandelier Tuff (Smith and Bailey, 1966, 1968). By comparison, the amount of ash released during the May 1980 eruptions of Mount St. Helens is estimated at 0.5 mi^3. From this vantage point, we can gaze southwest across Valle Grande, the eastern section of the caldera "moat", toward the broad mountain of Redondo Peak (11,254 ft) forming the eastern segment of the resurgent dome (Fig.

FIGURE 2.2. Oblique aerial view of northern Valle Grande, looking southwest. Location of Stop 1 on a flow lobe of Cerro del Medio rhyolite, is shown by the 1. SM, LJ, RP and R are South Mountain, Cerro La Jara, Redondo Peak and Redondito, respectively.

2.2). This segment is really a northeast-trending ridge that includes the small knob of Redondito. The resurgent dome is composed primarily of densely welded Bandelier Tuff that was uplifted during post-caldera tumescence of the volatile-depleted Bandelier magma chamber (Smith, 1979). Resurgence probably occurred about 50-100 ka after caldera formation (Doell et al., 1968; Smith and Bailey, 1968; Hulen et al., 1987). The stages of caldera formation and resurgence as proposed by Smith and Bailey (1968) are shown in Figure 2.3.

The Bandelier Tuff(s), particularly the Tshirege Member, is an excellent example of a chemically and mineralogically stratified ignimbrite produced from a compositionally zoned magma chamber (Smith andBailey, 1966; Smith, 1979; Stix et al., 1988). Warshaw and Smith (1988) reported that the basal Tsankawi Pumice, representing the top of Bandelier chamber, formed at a pre-eruption temperature of about 700°C, whereas the uppermost Tshirege ignimbrite formed at about 850°C. Several authors have indicated that the top of the Bandelier chamber was at 3–4.5 mi depth at eruption (Sommer, 1977; Neilson and Hulen, 1984; Warshaw and Smith, 1988). Smith (1979) indicated that the Bandelier chamber formed from parental magma resembling slightly older Tschicoma dacite. More recent geochemical investigations have shown that the Bandelier magma system has evolved by fractional crystallization of mantle basalt accompanied by only 10-30% assimilation of lower crust (DePaolo et al., 1992; Perry et al., 1993; Spell et al., 1993).

Visible post-caldera, ring-fracture rhyolites of the Valles Rhyolite that partly surround the resurgent dome are Cerro del Medio, Cerro del Abrigo (0.97 Ma), Cerro La Jara (0.52 Ma), and South Mountain (0.52 Ma) (Spell and Harrison, 1993). These rhyolites range from crystal-poor (Cerro del Medio) to coarsely porphyritic (South Mountain) but all are high-silica rhyolites. Geochemical data presented by Spell and Kyle (1989) and Spell et al., (1993) also show affinities to mantle basalt but suggest that each moat rhyolite developed uniquely.

Geothermal development and the cooperative agreement between Union Geothermal Co. and the U.S. Department of Energy have provided drill-hole and geophysical data

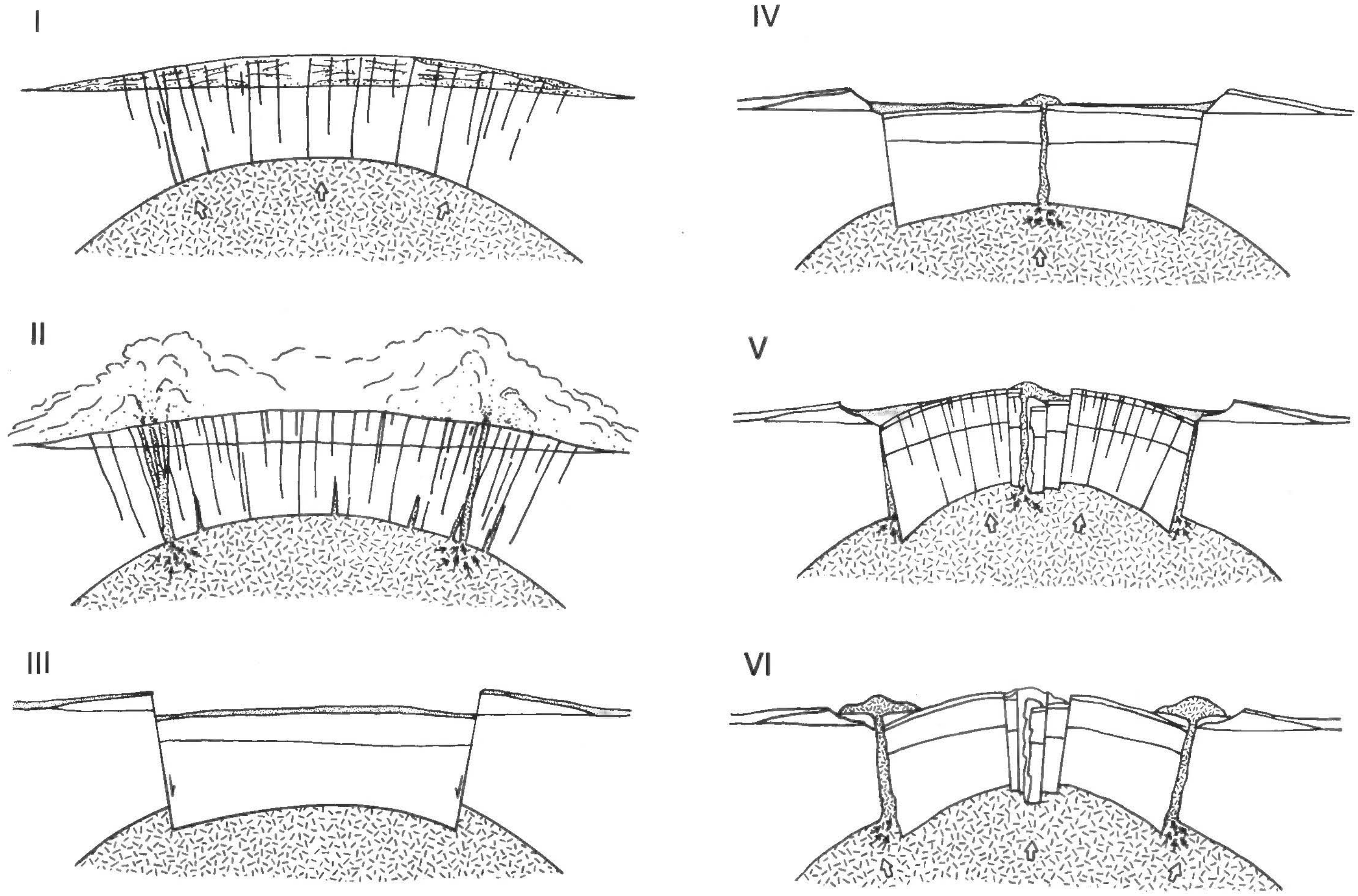

FIGURE 2.3. The six stages of caldera formation and resurgence in the model of Smith and Bailey (1968). I, Regional tumescence and formation of incipient ring fractures. II, Large volume ignimbrite eruptions. III, Caldera collapse. IV, Preresurgence volcanism and sedimentation. V, Resurgent doming. VI, Major ring fracture volcanism.

that give an interesting picture of subsurface caldera structure. Gravity data shows a broad, circular gravity low (35 mgals) due to low-density fill. The gravity models of Segar (1974) and Nowell (this volume) indicate that the floor of the caldera is very asymmetrical, being shallow on the west and deep on the east. These models are verified by drill-hole data in the western and central caldera. The models also indicate northeast-trending gravity gradients that are probably related to pre-caldera structures inherited from the Rio Grande rift (Nielson and Hulen, 1984; Heiken et al., 1986; Self et al., 1986; Aldrich, 1986; Goff et al., 1989). Depth to Precambrian basement rocks beneath Valle Grande is estimated at 13,000 ft (Nowell, this volume).

Regional seismic data (Gardner and House, 1987) shows that the caldera depression is seismically quiet compared to fault zones located outside the caldera (i.e., Pajarito fault zone; Jemez fault zone). Attenuation of seismic waves was first recognized by Suhr (1981). Olsen et al. (1986) implied that the large gravity low of the caldera and associated time-term delays were caused by residual melt in the Bandelier pluton. Ankeny et al. (1986) applied a simultaneous inversion of earthquake and travel-time data and modeled a prominent, low-velocity, cylindrically shaped body beneath the caldera that is 9 mi in diameter and 7.5–9 mi thick. This body was interpreted to result from the combined effect of a silicic magma chamber and associated high temperatures and was centered beneath the southwestern sector of the caldera.

Quantitative results of forward modeling applied to travel time delays for teleseismic P wave first arrivals show that a lens-shaped low-velocity zone (LVZ) underlies the center of the resurgent dome (Roberts et al., 1991, 1995). The width of the LVZ from tip to tip is 10.5 mi and the depth to the center of the anomaly is 6–8 mi. The thickness cannot be less than 5 mi and the P wave velocity is 3.5-4.2 km/s. Roberts et al. suggested that the LVZ results from a region of partial melt representing the present Bandelier magma chamber. (Fig. 2.4).

Valle Grande volcaniclastic and lacustrine deposits were described by Conover et al. (1963) and Griggs (1964) from surface exposures and several exploratory water wells. About 200 to 300 ft of pumiceous clay overlies at least 900 ft of pumiceous sand and gravel. The deepest well (1184 ft) did not penetrate volcanic rocks in the caldera moat. Wells in Valle Grande are artesian due to the clay-rich cap and the capacity of the wells are high (≤2800 l/min or ≤750 gpm). Based on stable isotope evidence, the northern and eastern moat zones of Valles caldera serve as recharge areas for reservoir fluids in the geothermal system (Vuataz and Goff, 1986). This is verified by heat flow data which shows a low relative heat flow due to downward circulation of cold meteoric fluids in this area of the

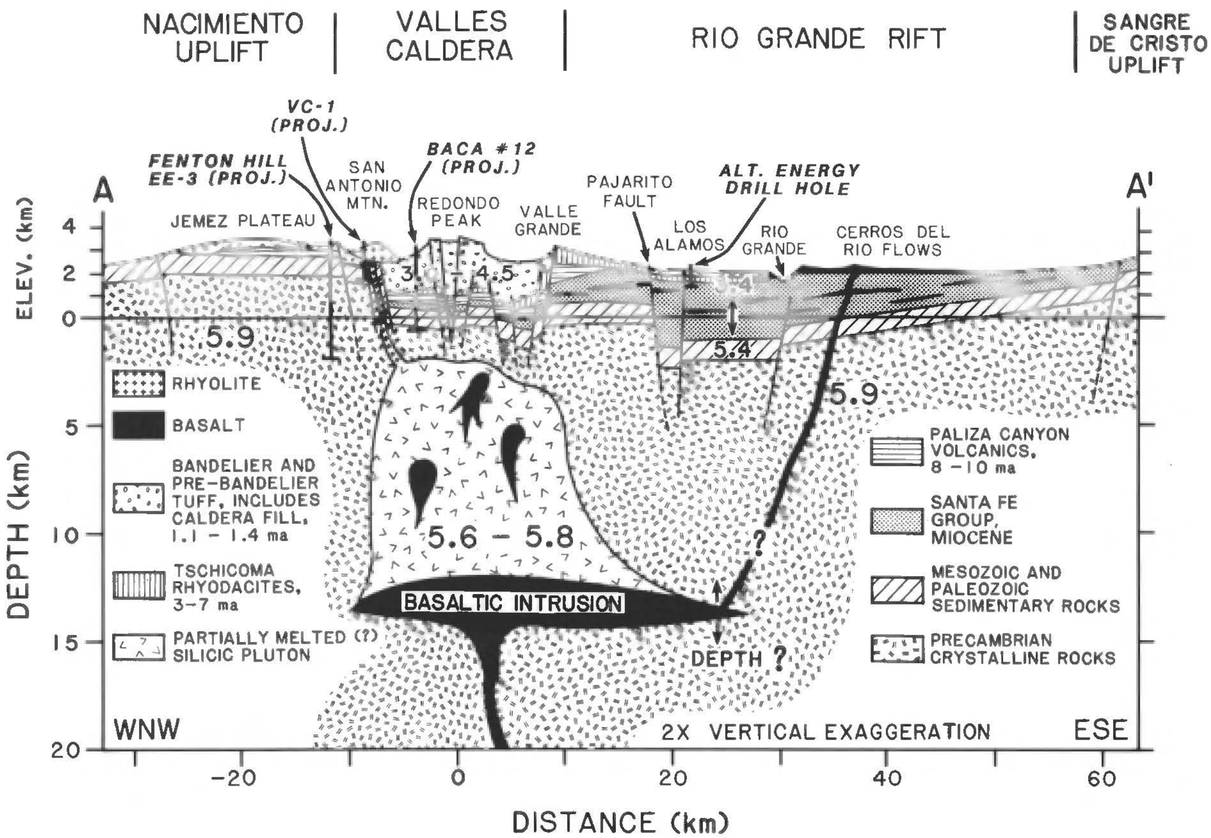

FIGURE 2.4. Schematic cross section through the Valles caldera and adjacent Rio Grande rift, showing the three-dimensional inversion interpretation of Ankeny et al. (1986). Seismic velocity values (large numbers) in km/sec are averages determined from the inversion technique.

caldera (Sass and Morgan, 1988; Morgan et al., this volume).

Continue east and then north around flow lobe of Cerro del Medio. **0.3**

16.4 Pajarito Mountain at 12:00, Sierra de los Valles at 3:00. **0.1**

16.5 On left, devitrified rhyolite colluvium of margin of Cerro del Medio flow. **0.1**

16.6 Begin descent into Rincon de los Soldados, site of the "famous" Rincon skirmish in which Indians captured the horses of U.S. Army hay providers in the late 1800s (Fig. 2.5). **0.2**

16.8 Cross headwaters creek of East Fork, Jemez River, and go through gate. **0.2**

17.0 On right, dacite domes of Tschicoma formation in the Sierra de los Valles, the eastern rim of the caldera. Pajarito Mountain at 1:00 and Cerro del Medio to left. **0.5**

17.5 On left, road cut into colluvium of rhyolite flow breccia off of Cerro del Medio. Vapor phase crystals in vugs in rhyolite and flow banded rhyolite. On right, East Fork of Jemez River. **0.4**

17.9 On right, at 3:00 is Pajarito Mountain, with gas pipeline through notch on left side of Mountain. Cerro del Medio on left. **1.2**

19.1 Pass through gate; pond on right; head of the Valle Grande. **0.4**

19.5 Crest of hill, begin descent into Valle de los Posos and headwaters of San Antonio Creek; from 10 to 11:00 is the southeastern dome of the Cerros de los Posos, now believed to be part of the Cerro Toledo Rhyolite; at 12:00 is Cerro Rubio, a remnant of a Tschicoma dacite dome. **0.3**

19.8 On right, pile of Tschicoma dacite rubble derived from east caldera wall. Northern rim of caldera on skyline at 9:00; Cerros del Abrigo on skyline at 8:00; Cerro del Medio in foreground from 6:00 to 9:00; northwestern Cerros de los Posos dome at 10:00; southeastern Cerros de los Posos dome at 11:00; Cerro Rubio at 12:00. **0.5**

20.3 Turn left at junction with Pipeline Road; dramatic cliffs of Tshirege Member, Bandelier Tuff, on northeastern rim of caldera from 12:00 to 1:00. **0.4**

20.7 On right, San Antonio Creek. Cerro del Medio is at 9:00, Cerros del Abrigo (part of the Valle Grande Member of the Valles Rhyolite) is at 10:30, north caldera wall is at 12:00, and southeastern dome of Cerros de los Posos is at 2:00. Toledo embayment is beyond Los Posos domes. **0.1**

20.8 Cross concrete culvert and cross several other metal culveretts for next 0.4 mi. **0.4**

21.2 Culvert. Begin to cross northeastern flow lobe of Cerro del Medio. Aphyric obsidian facies in Cerro del Medio rhyolite is slightly spherulitic. At 3:00, domes of Cerro Toledo Rhyolite can be seen between the southeastern and northwestern Cerros de los Posos domes. **0.1**

21.3 Gas line marker at top of hill on right. **0.4**

21.7 Small hairpin curve as road crosses a dry creek. **0.3**

22.0 On right, boulders of glassy, flow-banded Cerro del Medio rhyolite. Cross small creek. At 3:00, northwestern Cerros de los Posos dome. **0.1**

22.1 Cross T-junction with small road which comes through slot (Puerto de Abrigo) between Cerro del Medio and Cerros del Abrigo. **0.8**

22.9 Cross spring-fed creek that flows from Puerto de Abrigo; at 10:30 is Cerros del Abrigo, at noon is flow lobe from

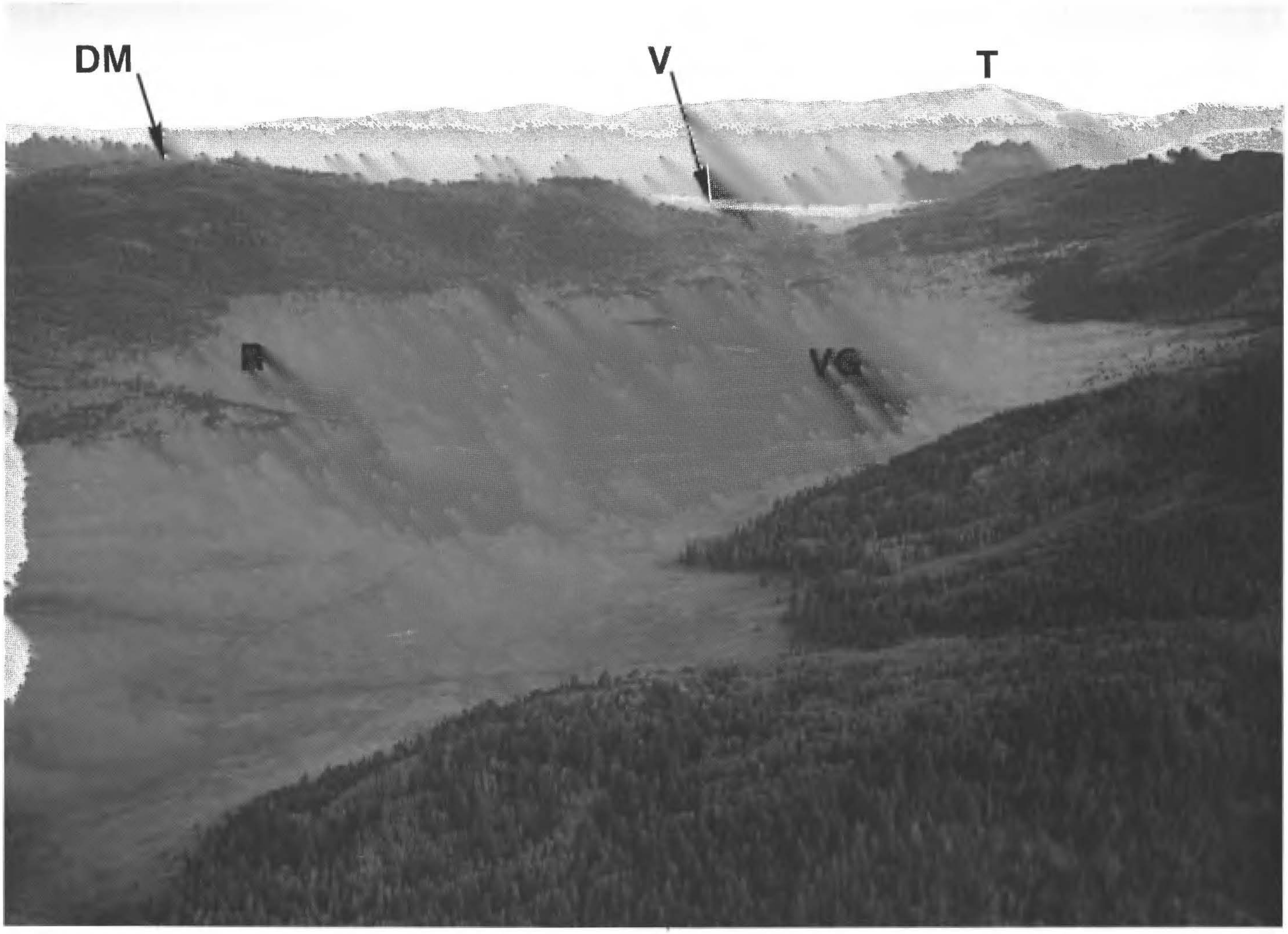

FIGURE 2.5. Oblique aerial view looking north-northwest across Valle Grande (VG) and the headwaters of the East Fork, Jemez River into the Toledo Embayment. DM is Cerro del Medio, V is an unnamed valley that connects Valle de los Posos to the east (right) with Valle Toledo to the west (not visible in this photo), T is Tschicoma Peak on the northern rim of the Toledo embayment, and R is Rincon de los Soldados.

Cerros del Abrigo, at 12:30 to 2:30 is Turkey Ridge, consisting of coalesced, eroded Cerro Toledo Rhyolite domes and flows, and at 2:00 (behind Turkey Ridge on skyline) is Cerro Toledo (with bald spot), for which the formation Cerro Toledo Rhyolite is named. **0.2**

23.1 Panorama of Valle Toledo; driving on terrace. **0.1**

23.2 **STOP 2. Valle Toledo overlook and rhyolite flow lobe.** We are standing on a pumiceous rhyolite flow lobe that Smith et al. (1970) showed to be part of Cerro del Medio. Relatively fresh outcrops of the rhyolite can be found just south of the road. Doell et al. (1968) showed Cerro del Medio to be a composite dome, consisting of three lobes that are dated at 1.133 to 1.095 Ma (Spell and Harrison, 1993), whereas Cerros del Abrigo, to the south-southwest, consists of three lobes all dated at 0.973 Ma. The geology of this area and the northern moat of Valles caldera is discussed in some detail by Gardner and Goff (this volume).

From this vantage point (Fig. 2.6), we can look across

FIGURE 2.6. Panorama of part of the Valle Toledo and some of the Cerro Toledo Rhyolite domes filling the Toledo embayment. Note the prominent alluvial terrace across the middle of the picture. P is the northwestern Los Posos dome, TR is Turkey Ridge, CT is Cerro Toledo, and arrow points to the Rito de los Indios, which is incised along the northwestern margin of the Toledo embayment (see Gardner and Goff, this volume).

Valle Toledo to the northern rim of the caldera complex. North, across the valley, are domes of Cerro Toledo Rhyolite that fill the Toledo embayment. Smith (1979) and Stix et al. (1988) suggested that the geochemical trends among these domes and associated tephras record the restoration of geochemical zonation in the Bandelier Tuff magma chamber between the two major caldera-forming events.

Ross et al. (1961) and Smith et al. (1970) depicted the Toledo embayment on the northeastern margin ofthe Valles caldera as the Toledo caldera, from which some 95 mi^3 of Otowi Member of the Bandelier Tuff was erupted at about 1.61 Ma (see also Smith and Bailey, 1966; Smith, 1979; Izett and Obradovich, 1994). Several lines of evidence, however, indicate that the Toledo caldera is nearly coincident with the younger Valles caldera, and that the Toledo embayment represents some older structure (see Self et al., 1986; Heiken et al., 1986; Gardner and Goff, this volume; Nowell, this volume). This evidence includes isopachs and implied source location for the Guaje pumice (Self et al., 1986), radial distribution of the Otowi Member around the Valles caldera (Smith et al., 1970), a thick sequence of caldera-fill Otowi Member tuffs beneath the resurgent dome of Valles caldera (Nielson and Hulen, 1984; Hulen et al., 1991), and an arc of post-Toledo, pre-Valles age rhyolite domes in the northern moat of the Valles caldera (Goff et al., 1984; Heiken et al., 1986). Three domes of this arc, interpreted to have been erupted within the Toledo caldera ring fracture (Goff et al., 1984; Heiken et al., 1986; Goff et al., 1989), can be seen from this stop: the east and west Los Posos domes, to the north and east, and Trasquilar dome, barely visible in the northwest where San Antonio creek, flowing west, has cut a notch. Another of the domes of this Toledo caldera ring fracture arc is the next stop of today's trip. The early whole rock K-Ar dates on the Cerro Toledo Rhyolite domes (Goff et al., 1984; Heiken et al., 1986) have been nicely corroborated by recent Ar-Ar work; Spell (this volume) reports Ar-Ar dates on east Los Posos of 1.477 Ma, west Los Posos of 1.545 Ma, and on Trasquilar dome of 1.369 Ma.

Also visible from this vantage point are prominent strath terraces that are cut here on underlying lacustrine deposits. These terraces were mapped by Griggs (1964), and may record the alluvial bevelling that accompanied draining of intracauldron lakes from the northern part of the caldera (Gardner and Goff, this volume).

Continue straight ahead on Pipeline Road. **1.6**

24.8 Culvert, broken "dangerous curve" sign and dangerous curve at top of hill. **0.1**

24.9 Roadcut in alluvial terrace with rounded cobbles of varied rhyolite lithologies over lacustrine deposits. On left is Cerros del Abrigo; Trasquilar dome is at 12:00. Road descends into valley toward meandering San Antonio Creek. **0.2**

25.1 Roadcut on left is Cerros del Abrigo flow lobe composed of pumiceous, glassy rhyolite with pale pink quartz, sanidine and trace of biotite. **0.3**

25.4 Crest of hill is soft, pumiceous, perlitic flow lobe from Cerros del Abrigo covered with terrace gravels. At 11:30 is Cerro Santa Rosa, part of Cerros de Trasquilar. **0.3**

25.7 Drive through gate after which road bends left, crosses pipeline, and descends. San Antonio Creek is on left. Outcrops of rhyolite flow from Cerro Santa Rosa (part of the Valle Grande Member of the Valles Rhyolite) occur on both sides of road. It is a relatively aphyric, pumiceous rhyolite with sparse phenocrysts of quartz, sanidine, and biotite. **0.2**

25.9 Cross pipeline and Rito de los Indios. Cerro Trasquilar, a Cerro Toledo Rhyolite dome, is on right (see fig. 3 in Gardner and Goff, this volume). At road junction do not take first right. **0.1**

26.0 Take road that bears to the right and climbs over colluvium on the shoulder of Trasquilar dome; enter Valle San Antonio. This rhyolite is glassy to perlitic to devitrified, often forming distinctive prismatic to platy blocks, and contains sparse phenocrysts of quartz, sanidine and biotite. **0.9**

26.9 On right, hydrothermally altered colluvium (Keres and Polvadera Group rocks) from north caldera wall is covered by alluvial terrace. **0.5**

27.4 At 9:00, Cerro Santa Rosa, formed by two coalescing domes; at 10:00, Redondo Peak; at 11:00, Cerro San Luis (a dome of the Valle Grande Member); and at 12:00, Cerro Seco (another dome of the Valle Grande Member). **0.4**

27.8 On right, hydrothermally altered Paliza Canyon Formation andesite (?) in huge landslide block from north caldera wall. Across creek is flow lobe from Cerro Santa Rosa. **0.8**

28.6 On left, junction with the "road to Jaramillo" that leads to ranch headquarters. Road climbs up Valle Santa Rosa until it reaches crest between Cerros del Abrigo and Redondo Border and then descends into Valle Jaramillo, which opens into Valle Grande. **0.3**

28.9 On right, Tschicoma Formation dacite from landslide blocks off north caldera wall. **0.9**

29.8 On left, junction with small road that follows pipeline; view of Redondo Peak between Cerro San Luis and Cerro Seco at 9:00. **0.2**

30.0 On right, lake deposits (?) in roadcut with rounded cobbles and pebbles of fluvial material. **0.4**

30.4 Junction on left with road to Bathhouse Spring cabin, on east side of Warm Springs dome. Main road heads toward southwest side of valley. The spring rises in the bottom of a wood shed that is out of view on the south side of the small hill of rhyolite (Warm Springs Dome). The spring water (T=38°C) is representative of the dilute thermal waters that circulate in the western moat of the caldera (Goff and Grigsby, 1982). **0.2**

30.6 **STOP 3. Warm Springs Dome and hydromagmatic deposits.** Park to the side of the road, and enjoy a short five minute walk to the knob south of the road. Warm Springs dome (Fig. 2.7) is one of several Toledo caldera ring fracture domes that miraculously survived formation of the younger Valles caldera. Spell et al. (this volume) reports an Ar-Ar date on this dome of 1.263 Ma, indicating its eruption was not long before the Valles caldera-forming eruption of the Tshirege Member of the Bandelier Tuff at 1.22 Ma (Izett and Obradovich, 1992). Surrounding the north flank of the dome is a sequence of phreatomagmatic tephra that forms an apron of bedded pumice, crystal lapilli, and rare lithic fragments in a classic tuff ring about the dome. Pore spaces are partially filled with clear to brown opal. The rhyolitic magma contained phenocrysts of quartz, sanidine, biotite and rare hornblende. This tephra records the early stages of the dome-building eruptions through an intracauldron lake. Interest-

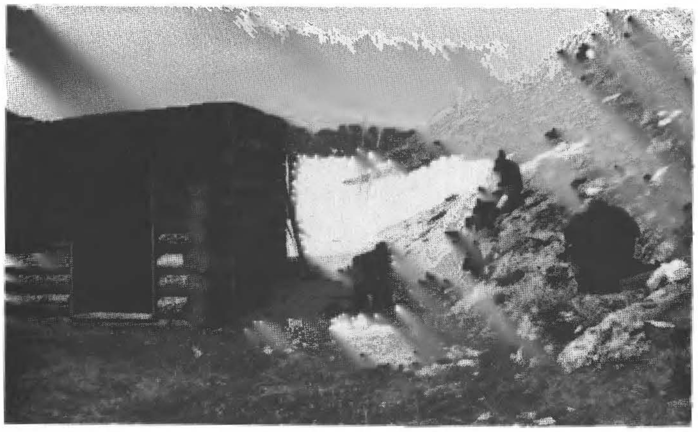

FIGURE 2.7. The bathhouse at Bathhouse Spring, at the edge of Warm Springs dome (hill at right), a Cerro Toledo Rhyolite, Stop 3.

ingly, Smith et al. (1970) showed that the Valles Rhyolite domes in the northern moat of Valles caldera are also partially surrounded by similar tuff rings. These tuffs are interbedded with the lake deposits.

Continue straight on Pipeline Road. **0.6**

31.2 Corral on right, plus landslide blocks off the north caldera rim. **0.2**

31.4 Cross San Antonio Creek. **0.2**

31.6 On left in roadcuts are interbedded fluvial and lacustrine deposits with overlying soil. **0.9**

32.5 Cross dry creek bed. To right is northwest wall of Valles caldera with huge landslide block. **0.2**

32.7 **STOP 4. Silicified lacustrine deposits.** In the shallow gully, just east of the road, silicified and laminated siltstones and pumiceous sandstones are exposed which were deposited from lakes (Fig. 2.8). Although many people envision a single, giant caldera-filling lake for the Valles caldera, it is evident that there were multiple intracauldron lakes that filled different parts of the caldera(s) at different times. Clearly, some of the Cerro Toledo Rhyolite (post-Toledo caldera) domes were being erupted through water ponded in the northern moat zone of the caldera, as indicated by the phreatomagmatic tuff ring that we saw at the last stop. Following formation of the Valles caldera, lakes that predated resurgent doming had formed, and left deposits that were involved in the structural doming event (Smith et al., 1970) within about 0.1 Ma of Valles caldera formation (Spell and Harrison, 1993).

Scientific core hole VC-2B, near Sulphur Springs on the west flank of the resurgent dome, penetrated 551 ft of interbedded accretionary lapilli tuffs, coarse clastic breccias, and fine-grained lacustrine rocks that are only gently tilted (10–15°) and exhibit hydrothermal alteration that predated soft sediment deformation (Gardner et al., 1989). These relations suggest that a lake, with very high bottom temperatures, formed in this part of the caldera soon after collapse, but postdating most structural doming, while the newly formed caldera walls and dome were shedding debris flows into the lake and small-volume eruptive activity continued.

Lake deposits in the northern moat of the caldera (in Valle San Antonio and Valle Toledo) appear to postdate the major mass wasting of the caldera walls, show depositional relations on rocks at least as young as 0.8 Ma, and are not structurally deformed (Smith et al., 1970; Spell and Harrison, 1993; Gardner and Goff, this volume). Griggs (1964) mapped flat-lying lake deposits in Valle Grande, and reported more than 1000 ft of caldera-fill deposits penetrated by a drill hole there. Some authors (e.g., Goff and Shevenell, 1987; Hulen and Nielson, 1988; Goff and Gardner, 1994) have suggested major breaching of the

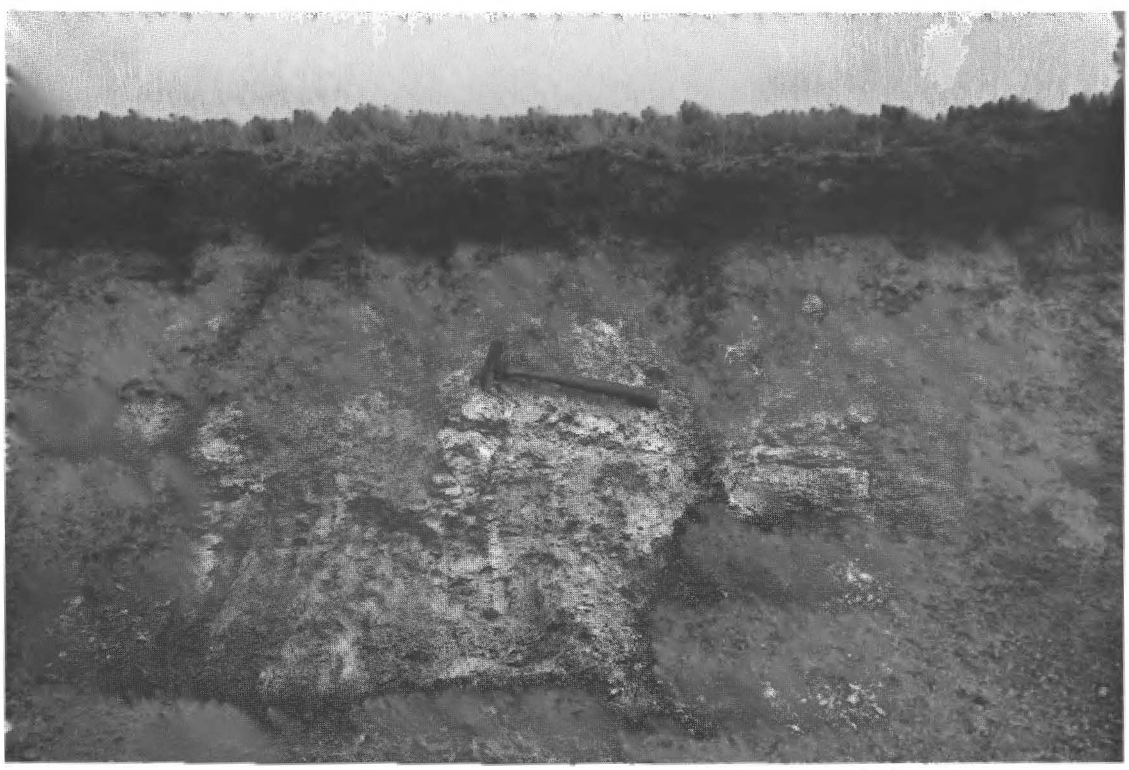

FIGURE 2.8. Tuffaceous lake deposits near Stop 4.

southwest caldera wall, rapid and deep incision, and dramatic changes in caldera hydrology, at about 0.5 Ma. This time, which is roughly coincident with large-volume dome eruptions in the southern and northwestern moats, apparently occurred when the lakes in the northern and western portions of the caldera drained rapidly, establishing the drainage patterns that persist today.

Turn left at the "Y" junction of roads. **0.2**

32.9 Cross cattle guard. Cerro Seco is at 11:00; San Antonio Mountain is at 1:00. Low hills on left are tephra deposits from Cerro Seco dome. **0.4**

33.3 On right, white, hydrothermally altered lacustrine rocks are exposed in gully. San Antonio Mountain rhyolite dome is to right. **0.5**

33.8 On left, Cerro Seco rhyolite flow overlies tephra. **0.9**

34.7 At drainage divide there is first an intersection with road on right, then with a road on left. Enjoy view over Valle Seco and of Redondo Peak (10:00) and Redondito (9:30); Cerro Seco is at 9:00 and San Antonio Mountain (another Valle Grande Member rhyolite dome complex) is at 2:00; begin descent into Valle Seco. **0.5**

35.2 Junction with small road to left; low hill of the Redondo Creek Member of the Valles Rhyolite is dead ahead. Sulphur Creek is on left. **0.2**

35.4 On left, flow-banded, hydrothermally altered, Redondo Creek rhyolite. **0.7**

36.1 Crude road to left; San Antonio Mountain to right. **0.8**

36.9 Cattle guard and road junction; **turn left** into Alamo Canyon. **0.1**

37.0 On right, green post marks site of Baca #2 geothermal well. This well was drilled in the early 1960s by James Dunigan, Baca Land and Cattle Company (Dondanville, 1971). It is significant because it encountered Precambrian rocks at about 5000 ft depth. Although the well achieved temperatures of about 200°C, flow was very minimal and the well was sub-commercial. **0.4**

37.4 Cold pond on right contains many gas seeps releasing about 98 mol-% CO_2, 1.5 mol-% H_2S, and 0.5 mol-% other gases. The pond is never hot enough to be considered thermal but reaction of gases with pond water causes formation of mildly acidic conditions (Goff et al., 1985). **0.2**

37.6 On right, green post marking the location of Baca #8 geothermal well (Hulen and Nielson, 1986b). This well intersected the Santa Fe Group (3120 ft) and bottoms in Permian Abo Formation (3448–4383 ft). Bottom hole temperature was about 280°C. Hydrothermal alteration is intense. Some zones contained altered horizons with 10% epidote. Metallic phases containing Ag and Br were found although the dominant metallic phase is pyrite. Although the well might have been a marginal producer, most wells in this area are not good so this area was never considered to be a prime production zone from the geothermal reservoir. **0.4**

38.0 On left, green post marks the site of Westates-Bond #1 geothermal well, the first deep hole drilled in the caldera (1959). At that time, the caldera property still belonged to the Bond family but was sold in 1960 to the Dunigan family. This well was really an oil and gas wildcat. Apparently, the west side of the resurgent dome was considered to be a potential trap for hydrocarbons. Instead of oil, the well struck water at temperatures of about 200°C and drilling was terminated because of dangerous production of steam and other drilling problems (Dondanville, 1971). Caldera-fill rocks including Bandelier Tuff extend to a depth of 2550 ft. Below this depth the rocks were described as "tuffaceous sand, silicified with secondary feldspar and pyrite." **0.1**

38.1 **STOP 5. Alamo Canyon geothermal features and Alamo bog.** Park on well pad. Green post marks site of Alamo Canyon #1 geothermal well and the large flat area was constructed for the drill rig, mud pits, logging trailers, and other support equipment. This well was drilled in 1979 by Union Geothermal to a depth of 7400 ft (Nielson, 1986), and penetrated welded tuff and caldera-fill rocks to 7284 ft, a considerably thicker sequence than in adjacent Westates-Bond #1. The Alamo Canyon fault mapped by both Smith et al. (1970) and Goff and Gardner (1980) runs E-W along the canyon and is probably responsible for this dramatic change in thickness. Another possibility is that Alamo Canyon #1 penetrated a possible vent area or significant topographic low in the pre-caldera topography.

A short (0.1 mile) walk to the east will bring you to Alamo bog, a series of shallow, cold ponds containing many gas seeps (Fig. 2.9). Some gas vents are so vigorous that you can hear them sizzle or hiss. Gas compositions are about the same as those down canyon; the odor of H_2S is strong. Pond fluids are mildly acid from oxidation of H_2S to H_2SO_4 but are otherwise quite dilute. Surrounding rocks are a caldera-fill sequence composed of hydrothermally altered to relatively fresh Bandelier Tuff (some pieces densely welded), pre-caldera volcanic rocks (mostly andesites and dacites), Santa Fe Group sandstone, Madera and Abo Formation limestone, siltstone, and sandstone. Very careful searching may reward one with a fragment of Precambrian basement, usually pink to red granite or gneiss.

For casual geologists, the presence of these various lithologies in the caldera fill is somewhat perplexing because they occur stratigraphically at several hundred feet depth below the caldera floor. Some intact blocks of pre-caldera rocks resemble rotated landslide blocks and may have slumped off the evolving caldera margin during caldera formation (Lipman, 1976; Lipman et al., 1989); the present caldera margin is about 1.8 mi west of us. Other zones of the caldera fill are chaotic; different patches of pre-caldera lithologies are found only feet apart. These

FIGURE 2.9. View of Alamo bog and hissing gas seeps, Stop 5.

characteristics and textural features in cores from recent wells suggest that pre-caldera rocks were explosively excavated from vent walls as the Bandelier Tuff was erupted and emplaced. The various pre-caldera lithologies were then incorporated in the ignimbrite.

In 1979, a 12.3-ft-long core was extracted from Alamo bog to determine environmental conditions during prehistoric times (Stearns, 1981). The bottom of the core ends in a peat layer (^{14}C age of 4595±105 y B.P.), indicating that additional sediments lie beneath the peat. Three more dates from the core were used to calculate sedimentation rates (about 3 in./yr near the bottom to about 12 in./yr near the top) and show that the rate has drastically declined in late Holocene time. Total abundance of pine and douglas fir pollen has decreased in the late Holocene, indicating a change to dryer conditions.

Turn around and retrace route. **1.0**

39.1 **Turn left** on Sulphur Creek road. **0.1**

39.2 On left, mouth of Short Canyon which contains more gas seeps and cold acid ponds and seeps. **0.4**

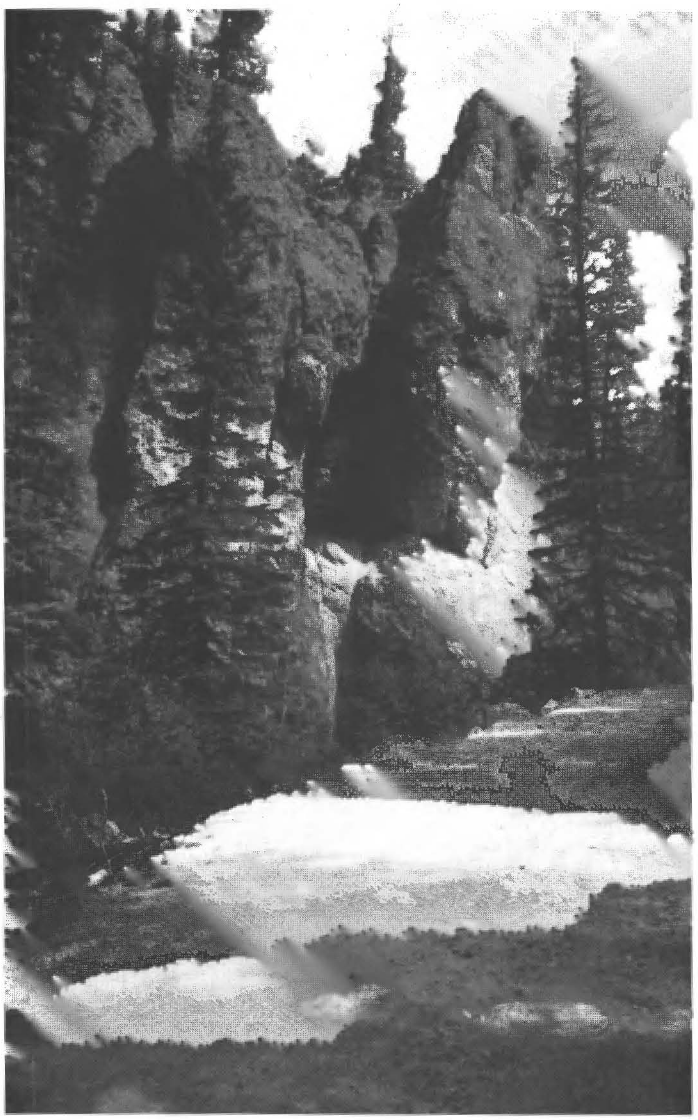

FIGURE 2.10. Massive flow breccia near the base of a flow of Redondo Creek Rhyolite. Some of these flow breccias are additionally cataclastically brecciated by movements on the Sulphur Creek fault.

39.6 Canyon displays hydrothermally altered, cataclastically brecciated, flow breccia of Redondo Creek rhyolite on both sides of road. Sulphur Creek fault zone is exposed on right (Fig. 2.10). **0.1**

39.7 Locked gate of Baca Ranch. **0.2**

39.9 On left, road to Turkey Flat and Continental Scientific Drilling Program (CSDP) corehole VC-2B. This hole was drilled from July to October, 1988 (Gardner et al., 1989) and is the deepest, hottest corehole in the conterminous United States. Total depth is 5780 ft and bottom hole temperature is 295°C. The hole penetrated the caldera fill sequence, a complete section of Tertiary through Paleozoic rocks, and several hundred feet of Precambrian quartz monzonite (Fig. 2.11). Core recovery is >99%. Several experiments were conducted in the well to obtain geothermal fluids and to test high-temperature slim hole tools (see Frontispiece to this volume). Alteration and vein minerals in the core include quartz, calcite, fluorite, illite, chlorite, epidote, anhydrite, anorthoclase, wairakeite, pyrite, chalcopyrite, sphalerite, pyrargyrite, rhodochrosite, and others (Goff and Gardner, 1994).

Depth to Precambrian basement in VC-2B is 5112 ft. Just west of the Sulphur Creek fault, beyond Sulphur Point, the WC23-4 geothermal well hit Precambrian rocks at 2418 ft; thus considerable offset occurs along ring-fracture faults and other faults going from west to east into the caldera depression. Maximum temperature in the WC23-4 well is 233°C at 6200 ft; thus temperature increases noticeably going into the caldera depression. Present convective heat flow is about 1,340±60 mW/m² (Morgan et al., this volume). **0.2**

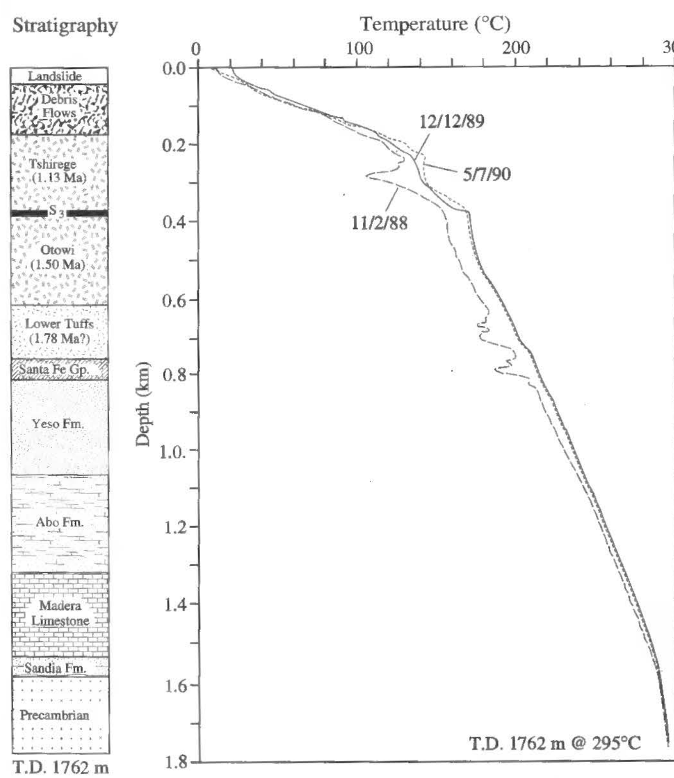

FIGURE 2.11. Stratigraphic section and temperature logs of Continental Scientific Drilling Program core hole VC-2B. The Tshirege Member, Otowi Member, and lower tuffs are caldera-fill facies, densely welded ignimbrites of the Bandelier Tuff. The Precambrian in VC-2B is biotite quartz monzonite.

RESERVOIR GEOCHEMISTRY FROM FLOW TESTS OF SCIENTIFIC CORE HOLES, SULPHUR SPRINGS, VALLES CALDERA

Cathy J. Janik[1] and Fraser Goff[2]

[1]Volcano Hazards Team, U.S. Geological Survey, Menlo Park, CA 94025;
[2]Geology/Geochemistry Gp., Los Alamos National Laboratory, Los Alamos, NM 87544

Core holes VC-2A and VC-2B were drilled in 1986 and 1988, respectively, as part of the U.S. Continental Scientific Drilling Program (Goff and Gardner, 1994). Scientific objectives were to delineate the vertical configuration of the hydrothermal system and to investigate the stratigraphy, structure, and hydrothermal alteration in the Sulphur Springs part of the Valles geothermal system. Technical objectives were to use diamond coring methods to obtain continuous core while achieving temperatures of about 200–300°C and to complete the holes such that they could be logged, flowed, and sampled for five years. Core samples are archived at the U.S. Department of Energy Core Repository in Grand Junction, Colorado (Starquist, 1988; Hulen and Gardner, 1989) and fluid samples are stored at Los Alamos National Laboratory and the U.S. Geological Survey (e.g., Goff et al., 1994).

Among the many investigations, flow tests were conducted to determine the chemical and isotopic composition of fluids at different horizons in the liquid-dominated system and to determine flow characteristics of the wells. At Sulphur Springs, the top of the liquid-dominated zone occurs at depths of roughly 490–550 m at temperatures of 190°C in fractured, intra-caldera ignimbrite that underlies the Otowi Member of the Bandelier Tuff ("lower tuffs", Hulen et al., 1991). Although temperatures increase to 295°C at 1762 m in Precambrian basement, temperatures in the water column are below the boiling point curve.

Most reservoir fluids circulate in fractured tuffs and underlying, semi-permeable sedimentary rocks of the Santa Fe Group. VC-2A produced fluid from one perforated horizon at 492 m and 210°C, whereas VC-2B produced fluids from five perforated horizons: 663 m, 196°C ("lower tuffs"); 686 m, 199°C ("lower tuffs"); 777 m, 207°C (Santa Fe Group); 989 m, 232°C (Yeso Formation); 1454 m, 282°C (Madera Formation). Before flow-testing VC-2B, fluids from the Precambrian interval were sampled by in-situ techniques (Goff et al., 1994), after which this interval was plugged. Shut-in pressures varied from 10–25 bars gauge depending on the well and the length of time the wells remained closed. The wells did not self-start when opened unless shut-in pressures were at their maximum values. In such situations, rapid depressurization on opening caused boiling at the top of the water column and immediate creation of two-phase conditions (vapor plus liquid). Flow commenced by geysering to heights of 5–20 m for a period of 1–3 min. After this initial period, flow changed to a continuous two-phase discharge that reached a height of over 30 m and roared like a jet engine. A light rain of brine and steam condensate fell around the well site. Because the brine in the reservoir is silica-rich (500 ppm SiO_2), this rain destroyed the windows and paint of any nearby vehicles by amorphous silica precipitation.

Once the wells reached steady-state conditions (usually in 15 min), the valves on the well heads were switched from top-flow to side-flow mode so that fluids were directed through a flow line to a weirbox (Fig. 2.12). The diameter of the flow line was slightly smaller than the diameter of the well casing (7.6 versus 10.2 cm diameter for VC-2B) to create back pressure. Well head temperatures during throttled flow of VC-2B were about 170–200°C. On the other hand, temperature in the weirbox was at the boiling point for surface pressure at this altitude (about 91°C at 2600 m). A V-notch at one end of the box allowed flow rate of "flashed" brine to be measured. Typical flow rates of VC-2B were about 70 L/min.

Small centrifugal steam separators were attached to sampling ports at two locations on the flow line (Fig. 2.12). The "mini-separators" were adjusted so that steam (vapor) and water (liquid) fractions were separated at known temperature and pressure into unique lines. Steam and water fractions were piped through a condenser (coiled tubing in pails of ice water) to cool the fluids below the boiling point for ease of sampling (Fig. 2.12). Water fractions were filtered, preserved with reagents (as required), and stored in a variety of glass and plastic bottles for later chemical analysis (Trujillo et al., 1987). Steam fractions were collected in special evacuated

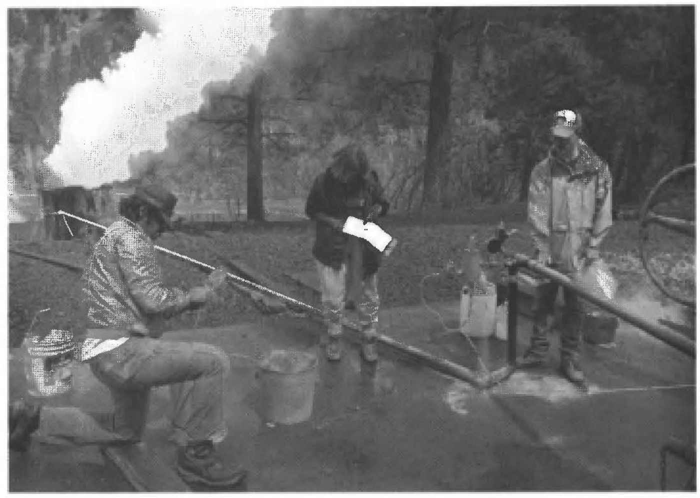

FIGURE 2.12. Sampling operations at VC-2B, May 11, 1992; first mini-separator (by standing man on right) is connected to left side of flow line that runs between well head (behind photographer) and weirbox (steaming in background). Mini-separator is adjusted to separate high-temperature fluid into vapor and liquid components. Sampling line and condensers (in the bucket) are connected to steam-side of separator. Man kneeling on left is collecting a gas sample.

bottles partially filled with 4N NaOH (Fahlquist and Janik, 1992). Acid components (CO_2, H_2S, NH_3) and condensed steam react and mix with the caustic solution, whereas non-acid gases (He, H_2, CH_4) fill the head space of the bottle (Fig. 2.12). Condensed steam samples were also collected from the steam line for chemical and isotopic analyses.

Detailed procedures for collecting samples and interpreting data obtained from flowing geothermal wells can be found in Janik et al. (1991). The basic equation of enthalpy or heat balance for a geothermal reservoir fluid is $H_r = y\ H_v + (1\text{-}y)\ H_l$ [1], where H_r is the enthalpy of the reservoir, H_v is the enthalpy of separated steam at separation temperature, H_l is the enthalpy of separated liquid at separation temperature, and y is the mass fraction of separated steam (e.g. Henley et al., 1984). Enthalpies of various components as functions of temperature are given in steam tables (Keenan et al., 1969).

The calculated steam fraction (y) has many applications. For example, the steam fraction at the weirbox of VC-2B is about 0.26 if the bulk reservoir temperature is estimated at 225°C and steam separation occurs at about 91°C. The total flow of the well (about 95 L/min) is calculated using $F_t = F_l / (1\text{-}y)$ [2], where F_t is the total flow (liquid plus vapor) and F_l is the measured flow of brine. Thermal power output, P, is determined from $P = F_t \Delta H$ [3], where ΔH is the difference between reservoir enthalpy and a "dead state" enthalpy. Using the ambient temperature of the area (10°C) for the dead state, the power output of VC-2B is about 1.5 MW(thermal).

The reservoir concentration, C_r, of conservative chemical components (those components that remain entirely in the liquid phase during boiling) is calculated from $C_r = C_l\ (1\text{-}y)$ [4], where C_l is the concentration in the separated liquid. For a sample collected at the VC-2B weirbox, the concentration of chloride (Cl^-) is 4050 ppm and the bulk concentration of Cl^- in the reservoir is therefore about 3000 ppm. Equation 4 is used to calculate reservoir concentrations for other relatively conservative components (SiO_2, Na^+, K^+, Mg^{2+}, Ca^{2+}, F^-, Br^-, SO_4^{2-}, and most trace elements) and for water-soluble residuals of volatile components (HCO_3^-, HS^-, NH_4^+).

Equations 1 and 4 can be used to check initial estimates of bulk reservoir temperature and composition by using data from the mini-separator samples. For example, the first mini-separator obtained a water sample at 175°C having a Cl^- content of 3240 ppm. The steam fraction is 0.111 and the calculated reservoir Cl^- content is 2880 ppm, about 4% lower than the value using weirbox data. On the other hand, the second mini-separator obtained a sample on the same day at 144°C having a Cl^- content of 3730 ppm, corresponding to a steam fraction of 0.169 and a reservoir Cl^- of 3100 ppm, about 3% higher than the weirbox value. The calculations indicate that the estimated bulk reservoir temperature of 225°C in VC-2B is probably accurate and that some fluid is contributed from all five horizons. For comparison, the 490 m interval in VC-2A has a Cl^- content of 2940 ppm whereas the Precambrian interval in VC-2B has a Cl^- content of about 4150 ppm (Goff and Gardner, 1994).

The concentration, C_i, of gaseous component i in the total-discharge fluid is calculated from

$$C_i = \frac{555.6\,(m_i M_i y x_g)}{1+yx_g} \qquad [5]$$

where m_i is the mole-% of gas i in the total gas, M_i is the molecular weight of gas i, and x_g is the molar gas/steam ratio. Volatile components in samples from the Sulphur Springs system consist of roughly 98.5 mole-% CO_2, 0.75 mole-% H_2S, and 0.75 mole-% others. CO_2 content in the total discharge varies from about 1100–12,800 ppm depending on depth of fluid entry. The in situ composition of the bulk reservoir fluid can be estimated by combining concentrations of gas and liquid components calculated from Equations 1, 4, and 5.

40.1 We are descending through toe of a large landslide complex. At 2:30 on skyline, outcrops of San Antonio Mountain rhyolite on Sulphur Point; lower slopes are Redondo Creek rhyolite. **0.1**

40.2 **STOP 6. Sulphur Springs and Well VC-2A.** Park along road or on short side roads and turnouts. Do not block traffic. Walk to left east to acid pond (Lake Corbin) and then walk up road to wellhead. Sulphur Springs was once a small resort where people bathed in the acid waters and mudpots to try to cure skin ailments. The resort burned down in the 1960s and nearly all of the original facilities have disappeared (Fig. 2.13). Rocks in this area consist of highly altered caldera fill sequence (Bandelier Tuff and exotic blocks) overlain by post-caldera rhyolites and associated rocks (Smith et al, 1970; Goff and Gardner, 1980). Ignimbrites of intracaldera Bandelier Tuff contain abundant small phenocrysts of quartz and sanidine. The narrow hill astride the main road consists of rhyolitic, hydromagmatic deposits which overlie caldera fill sequence; close examination shows beds with large accretionary lapilli and beds with sandstone fragments resembling Santa Fe Group and Abo Formation. The bluff south of the springs and the lower slopes to the west are formed of Redondo Creek Rhyolite (about 1.0 Ma). This unit consists of flows produced from several vents that erupted during growth of the resurgent dome (Smith and Bailey, 1968). It is very distinctive because it contains phenocrysts of plagioclase, biotite, and rare pyroxene, but no quartz. Sulphur Point to the west is formed of San Antonio Mountain Rhyolite (a moat rhyolite dated at about 0.5 Ma) and is a coarsely porphyritic rock with phenocrysts of quartz, sanidine, plagioclase, biotite, pyroxene, and rare hornblende. Near-surface alteration is argillic to advanced argillic due to low-temperature (100°C) attack of silicic rocks by acidic fluids (Charles et al., 1986). Typical alteration minerals are kaolinite, alunite, silica phases, and pyrite laced with native sulfur. A large landslide complex occurs to the north and east.

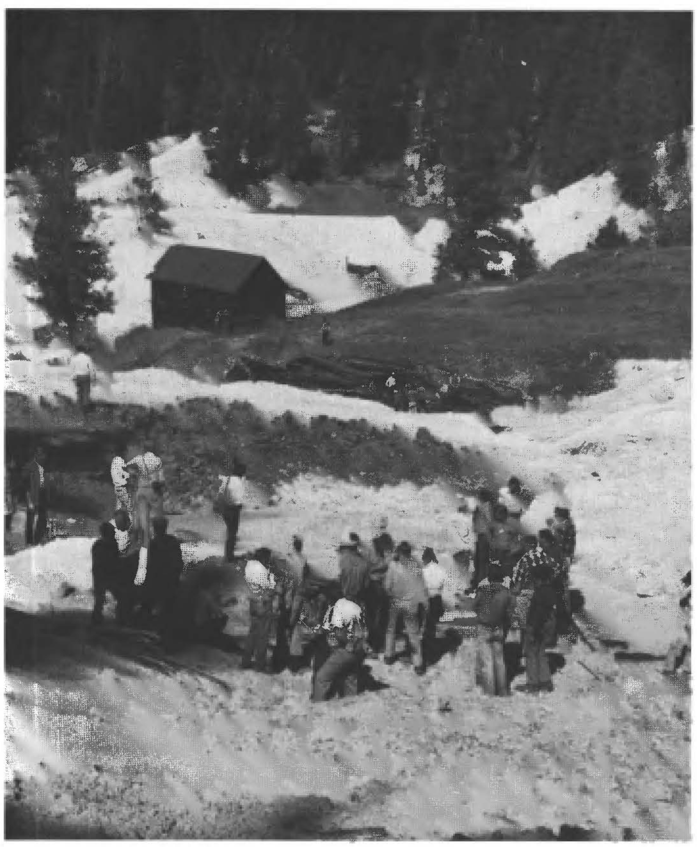

FIGURE 2.13. View looking north from Women's Bathhouse Spring (90°C) toward the main area of Sulphur Springs. Men's Bathhouse Spring (75°C) lies under a pile of lumber from the fallen old bathhouse (right of the cabin). Note bleached appearance of the rocks that have been altered by the acid-sulfate waters.

Thermal features occur at the intersection of the northeast-trending Sulphur Creek fault and several cross-faults (Goff et al., 1985). Fumaroles, mudpots, and hot and cold acid springs discharge on these structures. Temperatures range from background to 91°C, the boiling temperature at 8300 ft. Chemically, the springs are natural sulfuric acid waters; SO_4 contents may reach 10,000 ppm and pH may be <1. Dry gas consists of 98 mol-% CO_2, 1.5 mol-% H_2S, and 0.5 mol-% other (H_2, He, CH_4, NH_3, N_2, etc.). Empirical gas geothermometry indicates that gas originates from boiling of the 215°C reservoir fluid. Wells drilled in this area have extremely low formation pressures (0.76 MPa or 110 psi) to depths of roughly 1650 ft. Present convective heat flow is 7200±370 mW/m^2 (Morgan et al., this volume).

CSDP corehole VC-2A (Fig. 2.14) was drilled in September 1986 about 150 ft from Footbath Spring (Goff et al., 1987; Hulen et al., 1987). The hole is 1732 ft deep and has a bottom temperature of 212°C. All rocks penetrated are intracaldera tuffs and associated breccias and volcaniclastic sedimentary rocks (Hulen et al., 1992). The configuration of the Sulphur Springs hydrothermal system consists of an acid-sulfate condensation layer no more than 16 ft thick, a vapor zone extending to roughly 800 ft depth, a zone of fractured but tightly sealed rock from 800 to 1600 ft, and a liquid-dominated geothermal reservoir below 1600 ft. Fluids from the 1600 ft zone (210°C) are Na-K-Cl in composition as are all geothermal reservoir fluids in the caldera (Goff and Gardner, 1994). Fluids are about 2000 to >10,000 yrs in age depending on position within the reservoir (Shevenell and Goff, 1995; this volume). ^{36}Cl isotope work indicates that the Cl is primarily leached from Paleozoic and Precambrian rocks underlying the caldera (Rao et al., 1996; this volume).

Shallow sub-ore molybdenite (MoS_2) mineralization was penetrated by VC-2A from 80 to 400 ft in quartz-sericitized intracaldera ignimbrite (Fig. 2.15). The "moly" is an un-

FIGURE 2.14. Photo of VC-2A erupting flashed reservoir fluid from a depth of about 1,600 ft on May 1, 1987, while Lisa Shevenell and landowner John Corbin gaze in awe. Reservoir temperature at this depth is 210°C. The alkaline chloride reservoir fluid has dramatically different chemistry than the acid-sulfate springs at the surface.

usual, poorly crystalline variety that occurs in vuggy veinlets and breccia cements. Associated minerals are quartz, fluorite, illite, pyrite, chalcopyrite, sphalerite and rhodochrosite. Fluid inclusion data indicate that this assemblage was deposited from dilute fluids (0.2–0.5 equivalent wt-% NaCl) at temperatures ≤240°C. Because the molybdenite mineralization was deposited from liquid water but now occurs in a zone where low-pressure vapor fills fractures, the surface of the liquid-dominated reservoir has descended since the deposit was formed (Goff et al., 1987: Hulen et al., 1987; Gardner and Goff, 1994; Sasada and Goff, 1995). Illite in the molybdenite zone has K-Ar ages of 0.66 Ma (WoldeGabriel and Goff, 1989); thus the present vapor zone is younger than this age. Intense hydrothermal activity has affected magnetism in the intracaldera tuffs (Geissman and Mullally, this volume).

Continue straight ahead. **0.3**

40.5 On right, hydrothermally altered flow and flow breccia of Redondo Creek rhyolite. **0.2**

40.7 Pass through locked gate. Leaving Sulphur Springs and Baca Ranch and entering Santa Fe National Forest land. **0.6**

41.3 Bridge over Sulphur Creek. **0.3**

41.6 On left, driveway to private residences and mouth of Freelove Canyon. **0.6**

42.2 Cattle guard; entering Rancho de la Cueva, site of many homes. **0.1**

42.3 On left, Lark Road and mouth of Deer Canyon. **0.1**

42.4 On left is Elk Trail Road and the skyline of Redondo Border. V-cuts are NE-trending faults. Re-entering Santa Fe National Forest. **0.2**

42.6 On right is junction with Thompson Ridge Road. The WC

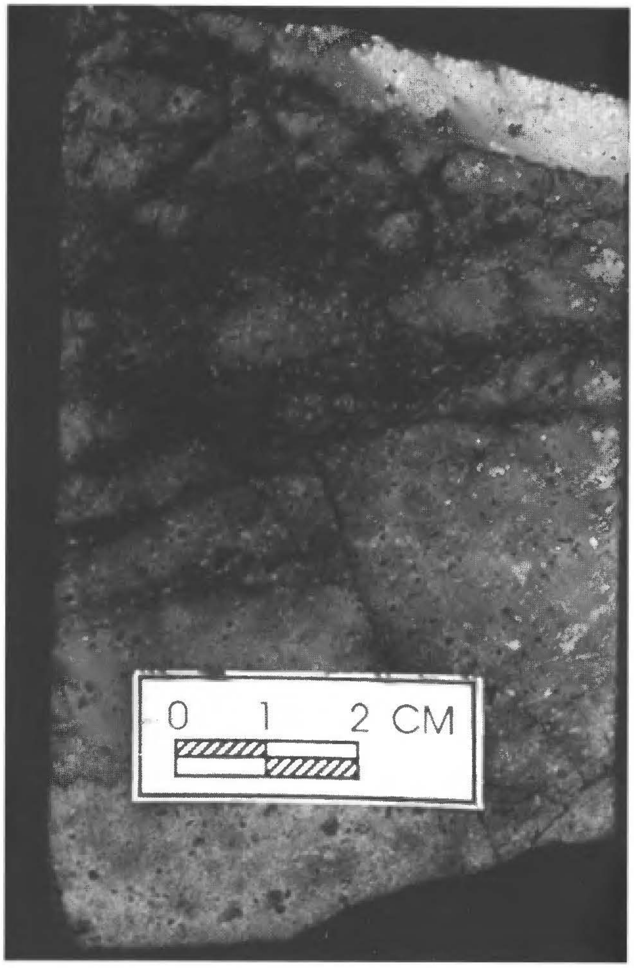

FIGURE 2.15. Slabbed and polished core sample of fractured, quartz-sericitized, intracaldera welded tuff with breccia cement of molybdenite, from a depth of about 100 ft in VC-2A. The molybdenite is associated with pyrite-quartz-illite-fluorite and trace sphalerite-chalcopyrite-rhodochrosite. Illite from this zone has a K-Ar age of 0.66 Ma. Maximum fluid inclusion homogenization temperature is 200°C, but present temperature is about 90°C and open fractures contain low-pressure vapor. (Core diameter is 2.5 in.; photo is courtesy of J. B. Hulen).

23-4 geothermal well (232°C at 6200 ft) is about 1.25 mi up the road (Goff et al., 1985). **0.2**

42.8 Stop sign. Intersection with NM-4; **turn left** and cross Sulphur Creek. After turn, Redondo Border is at 12:00, Redondo Peak is at 1:00. **0.3**

43.1 **Turn left** onto Redondo Creek road. **0.4**

43.5 Pass through locked gate and drive past old Union Geothermal Company guard station into Redondo Creek area; re-entering Baca Ranch. On right is Redondo Creek and behind it the Banco Bonito rhyolite flow. On left is southwest nose of Redondo Border, which comprises the western segment of the resurgent dome. Redondo Border is composed primarily of caldera-fill rocks and intracaldera Bandelier Tuff. **1.2**

44.7 **Turn left** at junction just before cattle guard; Redondo Peak at 1:00; Banco Bonito vent at 2:30 (low hill at south end of Redondo Peak); Redondo Border on left. **0.7**

45.4 Drive through old gate. **0.9**

46.3 On left, green post marks site of Baca #12 geothermal well (Fig. 2.16). This is the deepest and hottest well in the geothermal field (10,532 ft) and has a bottom hole temperature of 342°C (Nielson and Hulen, 1984). Altered Precambrian granite was encountered at 10,171 ft. The well was sub-commercial and was deepened into the Precambrian to explore for deep permeability but none was found. Alteration in Paleozoic strata includes hydrothermal biotite, diopside and tremolite (Hulen and Nielson, 1986a). **0.2**

FIGURE 2.16. Wellhead of Baca Well #12, the deepest and hottest well drilled in Valles caldera. Intracaldera Bandelier Tuff is exposed (in background) in the walls of Redondo Creek graben.

46.5 Cross Redondo Creek and continue drive into Redondo Creek graben. **0.2**

46.7 On right, shell of Union Geothermal Company of New Mexico's company headquarters. **0.1**

46.8 Geothermal well pad on left. **0.4**

47.2 Large clearing appears on left. **0.4**

47.6 **Turn around** to come back to Stop 7. **0.4**

48.0 **STOP 7. Redondo Creek graben and Baca-6.** Park along road and walk into the broad clearing to right bounded by retaining walls. We are standing in the Redondo Creek graben, the "keystone" graben within the Valles caldera resurgent dome (Figs. 2.17–2.19). Redondo Peak to the east is 11,254 ft high. Redondo Border to the west is 9925 ft high. Rocks exposed along the walls of the graben are primarily intracaldera Bandelier Tuff with caldera-fill breccias and debris. A post-caldera vent for a flow of Redondo Creek Rhyolite occurs further up canyon.

Drilling results and gravity modelling (Segar, 1974; Nielson and Hulen, 1984; Heiken et al., 1986; Nowell, this volume) indicate that the subsurface structure of Valles caldera is considerably more complicated than the idealized model of resurgence. The caldera floor is cut by precaldera structures paralleling the trend of the Rio Grande rift and is much shallower on the west than in the east. The thickness of intracaldera ignimbrites is approximately two to three times greater than originally estimated from surface mapping (Smith et al., 1970). The earlier, coaxial Toledo caldera and its associated collapse also complicate the subsurface structure. Although the surface morphology of Valles caldera is very symmetrical, with a ring of moat rhyolites surrounding a central structural uplift, the subsurface structure is not symmetrical (see Fig. 2.1).

Thermal features in this graben are not as spectacular as those on the west side of the resurgent dome. Weak, argillic alteration is found in the rocks on either side of the valley (Fig. 2.20). Gas seeps are located sporadically along graben-bounding faults. Gases are released by subsurface

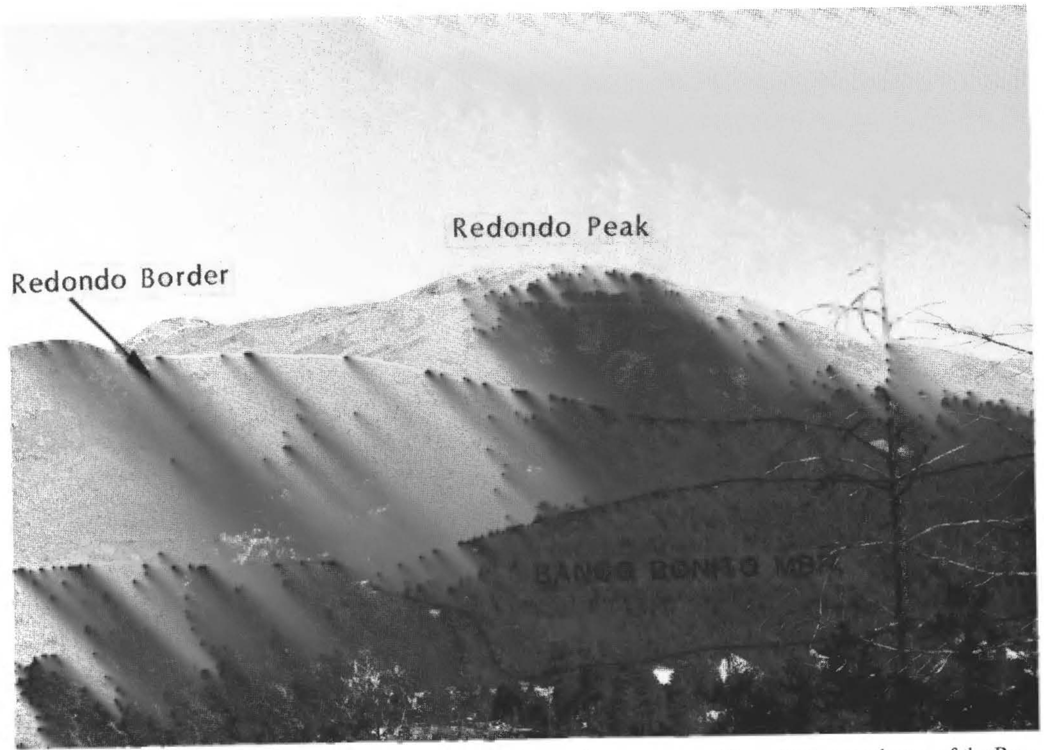

FIGURE 2.17. The resurgent dome of Valles caldera looking east-northeast from the southwestern rim of the caldera, over the toe of the Banco Bonito obsidian flow. Redondo Peak is on the southeastern flank of the dome, and Redondo Border forms the northwestern flank of the dome. The northeast-trending Redondo Creek graben separates the two flanks (see Fig. 2.18).

FIGURE 2.18. Oblique aerial view, looking northeast, of the Redondo Creek graben in the resurgent dome of Valles caldera. Bandelier Tuff can be seen dipping northwest on the northwest flank of the resurgent dome (Redondo Border, just to right of the airplane's wing strut). Redondo Peak is just to the right of the photo. The bare spots are well pads and other sites for the geothermal project of 1964–1984.

FIGURE 2.19. Panorama, looking southeast to south, of the southeastern segment of the resurgent dome of Valles caldera; Redondo Peak (11,254 ft above sea level) on the right, Redondito on left. The well pad for Baca-4, the "discovery" well for the geothermal system, is shown. The valley in the foreground is part of the Redondo Creek graben.

boiling from the underlying geothermal reservoir. Although Baca #6 was a marginal producer, other wells in this area (Baca #4, #13, #15, #19, #24) are the best in the field. Production temperatures were ≤280°C from depths of ≥3300 ft (Truesdell and Janik, 1986; White, 1986).

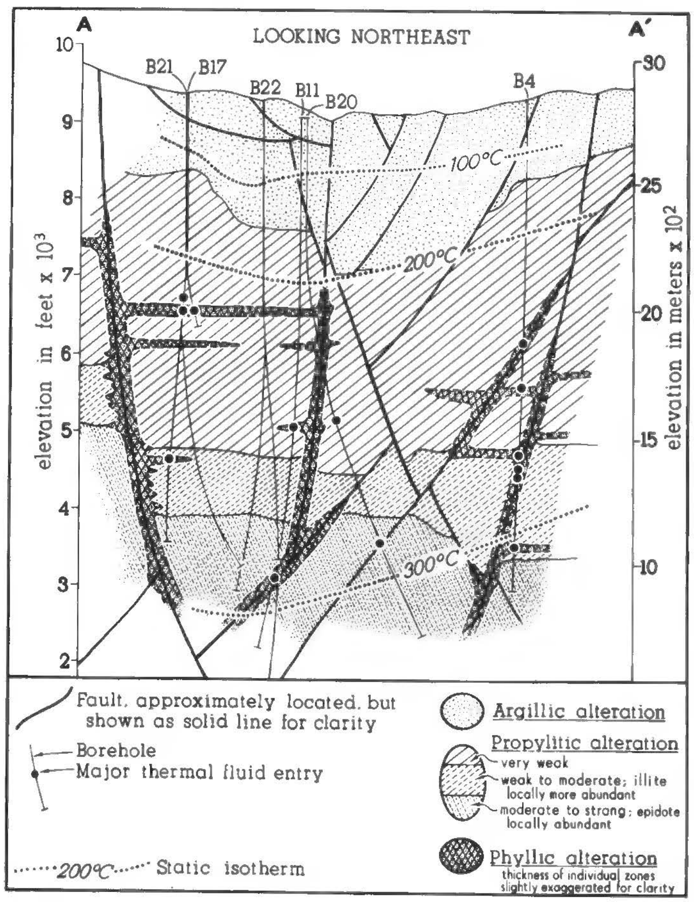

FIGURE 2.20. Generalized hydrothermal alteration cross section through the Baca geothermal system (from Hulen and Nielson, 1986a).

Geochemical data indicates that there are two types of reservoir fluid (Smith and Kennedy, 1985; Truesdell and Janik, 1986) in the Redondo Creek area. Best production is from or adjacent to graben-bounding faults (Hulen and Nielson, 1986a).

The large clearing was prepared in the early 1980s for construction of a 50 MW(e) geothermal power plant (Fig. 2.21). Union Geothermal intended to sell the electricity to the Public Service Company of New Mexico, but after drilling 24 wells over 20 years, only 20 MW(e) was proven. The project was terminated in 1984 because of the lack of permeability and reservoir volume, and the threat of lawsuits by various Indian pueblos over water-rights issues (Kerr, 1982; Goldstein and Tsang, 1984). The turbines intended for use at Valles caldera are now producing power at the Loa Azufres geothermal field in Mexico.

Return toward NM-4. **3.6**

51.6 Pass through locked gate (same as mile 43.5 coming in). **0.5**

FIGURE 2.21. View looking north up the Redondo Creek graben from the former site of the Baca-6 well (marked by the pole). The gravel embankment and concrete retaining wall were to protect the proposed 50 MW(e) geothermal power plant that was never built on this prepared pad. Arrow points to a group of people for scale.

52.1 Stop sign. **Turn left** at junction with NM-4. **End of Second-day road log.** We are now at Mile 81.0 of the Day 1 Road Log, and most of the remaining route to Los Alamos is detailed in that log. At Day 1 mile 103.5 turn left from NM-4 onto NM-501, and retrace our route from this morning, beginning at mile 4.8, back to our starting point at Sullivan Field.

Some buildings on the Baca Ranch. Upper photo is the "cowboy cabin" at Warm Springs dome in Valle San Antonio; lower photo is a movie set built in Valle Grande for the slapstick Western, "The Fight Before Christmas".